OXFORD

SOT | Society of Toxicology
www.toxsci.oxfordjournals.org

TOXICOLOGICAL SCIENCES, 159(1), 2017, 64–75

doi: 10.1093/toxsci/kfx117
Advance Access Publication Date: June 19, 2017
Research Article

Nlrp3 Is Required for Inflammatory Changes and Nigral Cell Loss Resulting From Chronic Intragastric Rotenone Exposure in Mice

Eileen M. Martinez,* Alison L. Young,* Yash R. Patankar,† Brent L. Berwin,† Li Wang,‡ Katharine M. von Herrmann,* Jaclyn M. Weier,* and Matthew C. Havrda*,[1]

*Department of Molecular and Systems Biology and †Department of Microbiology and Immunology, Geisel School of Medicine at Dartmouth, Lebanon, New Hampshire 03756; and ‡Department of Microbiology and Molecular Genetics, Medical College of Wisconsin, Milwaukee, Wisconsin 53226

[1]To whom correspondence should be addressed at Department of Molecular and Systems Biology, Geisel School of Medicine at Dartmouth, 1 Medical Center Drive, Lebanon, NH 03756. E-mail: matthew.c.havrda@dartmouth.edu.

ABSTRACT

Complex interactions between genetic and environmental factors are widely believed to underlie the incidence and progression of Parkinson's disease (PD). Rotenone is a naturally occurring metabolic toxin employed as an insecticide and piscicide identified as a risk factor for the development of PD in agricultural workers. The Nlrp3 inflammasome is an intracellular mediator that can initiate an inflammatory cascade in response to cellular stress. Reports by others indicating that *NLRP3* expression was detectable in tissues obtained from Alzheimer's disease patients and that the PD-associated protein α-synuclein could activate inflammasomes in cultured glial cells, prompted us to test the prediction that *Nlrp3* was required for the development of Parkinson's-like changes resulting from rotenone exposure in mice. We exposed wild type and *Nlrp3*$^{-/-}$ mice to chronic low doses of intragastric rotenone and conducted longitudinal behavioral and serum cytokine analysis followed by evaluation of neuroinflammatory and neurodegenerative endpoints in brain tissues. We observed progressive rotenone-dependent changes in serum cytokine levels and circulating leukocytes in wild type mice not observed in *Nlrp3*$^{-/-}$ mice. Analysis of brain tissues revealed *Nlrp3*-dependent neuroinflammation and nigral cell loss in mice exposed to rotenone as compared with mice exposed to vehicle alone. Together, our findings provide compelling evidence of a role for *Nlrp3* in nigral degeneration and neuroinflammation resulting from systemic rotenone exposure and suggest that the suppression of *NLRP3* activity may be a rational neuroprotective strategy for toxin-associated PD.

Key words: Nlrp3; inflammasome; rotenone; neuroinflammation; Parkinson's.

Parkinson's disease (PD) is the second most common neurodegenerative disorder affecting the elderly (de Lau and Breteler, 2006) and once clinical symptoms appear the disease has advanced beyond therapeutic interventions and physicians can provide only symptomatic treatments. There is no single animal model that fully recapitulates PD symptomology; however, there is an increasing interest in the analysis of slowly progressive genetic and epidemiologically relevant animal models where specific gene-environment interactions can be characterized (Blesa *et al.*, 2012; Duty and Jenner, 2011; Greenamyre *et al.*, 2010). The characterization of specific genes involved in translating systemic environmental toxin exposure into neuroinflammation and neurodegeneration is expected to aid in accelerating the development of sorely needed diagnostic strategies and neuroprotective therapies for PD.

Widespread use of the mitochondrial toxin rotenone to model PD in rodent and cell models emerged in part from genetic findings implicating mitochondrial dysfunction in the

development of PD (Abbas *et al.*, 1999; Canet-Aviles *et al.*, 2004; Valente *et al.*, 2004). This experimental effort was validated by large-scale epidemiologic studies implicating rotenone as a risk factor for the development of PD in agricultural workers (Tanner, 1989; Tanner *et al.*, 2011). In rats, consistent nigrostriatal degeneration is observed following infusion of physiologically relevant concentrations of rotenone using surgically implanted osmotic pumps (Betarbet *et al.*, 2000) and daily intraperitoneal injections (Cannon *et al.*, 2009). Mice represent a particularly attractive model system for evaluation of rotenone-mediated changes because they are more easily genetically engineered; a feature of importance given the likelihood that complex gene-environment interactions contribute to the development of PD (Cannon and Greenamyre, 2013; Dardiotis *et al.*, 2013; Ross and Smith, 2007; Singh *et al.*, 2014). Mice have proven more resistant to rotenone-induced toxicity compared with rats (Johnson and Bobrovskaya, 2015), however, multiple reports now indicate that long-term intragastric exposure to doses of rotenone ranging from 5 to 100 mg/kg can recapitulate behavioral and histopathologic aspects of PD in mice (Inden *et al.*, 2011; Pan-Montojo *et al.*, 2010). The analysis of genetically modified mice in the context of rotenone exposure will extend pioneering studies conducted in rats (Betarbet *et al.*, 2000) by helping to identify novel gene-environment interactions important in PD progression.

Neuroinflammation is a well-characterized histopathologic feature of PD (Hirsch and Hunot, 2009). The NLRP3-inflammasome is an intracellular inflammatory mediator that can initiate an inflammatory cascade in response to a variety of intracellular stress (Schroder and Tschopp, 2010). The NLRP3 inflammasome has been implicated in the pathogenesis of Alzheimer's disease (AD) (Heneka *et al.*, 2013) and recent animal studies indicated that mice lacking either *Nlrp3* (Yan *et al.*, 2015), or the key inflammasome effector *Caspase 1* (*Casp1*) (Qiao *et al.*, 2016), are resistant to nigral cell loss resulting from acute exposure to the neurotoxin MPTP. Zhou and others found that mitochondrial stress elicited by rotenone was able to activate the Nlrp3 inflammasome in association with elevated ROS in blood cells (Won *et al.*, 2015; Zhou *et al.*, 2011) and the PD-associated protein α-synuclein can activate inflammasomes in glial cells (Codolo *et al.*, 2013). Further characterization of *Nlrp3* in epidemiologically relevant PD models is of great interest because of its potential to act within a common pathway influenced by both disease-associated environmental toxins like rotenone and genetic risk factors for PD, many of which are also associated with mitochondrial stress (Klein and Westenberger, 2012).

Immunohistologic evidence of neuroinflammation in cranial nerves (Pan-Montojo *et al.*, 2010) is observed in association with enteric α-synuclein pathology and the progression of PD symptoms following intragastric exposure to 5 mg/kg rotenone for 3 months (Pan-Montojo *et al.*, 2012). We extended this low-dose exposure period to 6 months, gavaging 5 days per week to mimic typical occupational exposure and ensure that animals would survive for extended time periods (Cannon *et al.*, 2009; Drolet *et al.*, 2009). In this system, we characterized systemic and neurologic inflammation in mice lacking *Nlrp3*. We provide independent validation of this model system and present findings indicating that *Nlrp3* is required for systemic and neurologic inflammatory changes and loss of dopaminergic neurons in the substantia nigra pars compacta (SNpC) resulting from intragastric exposure to rotenone. Mechanistic studies provide evidence of a role for *Nlrp3* in mediating microglia-dependent induction of astroglial Cxcl1. These findings support a role for *Nlrp3* in mediating toxin-induced inflammation and parkinsonian neurodegeneration in mice and suggest that further characterization of *Nlrp3* function in this model system will improve our understanding of the cellular and molecular progression of PD.

MATERIALS AND METHODS

Research Animals and Rotenone Exposure. All animal studies we describe were conducted in accordance with federal guidelines and approved by the Dartmouth Institutional Animal Care and Use Committee. Wild type, *Nlrp3*$^{-/-}$, *Casp1*$^{-/-}$, and *IL1R*$^{-/-}$ animals were of C57/B6 genetic background and male and female animals were included in each cohort. Rotenone exposure was conducted as previously described (Pan-Montojo *et al.*, 2010). Briefly, intragastric gavage was utilized to deliver 5 mg/kg rotenone or vehicle (5% Hydroxypropyl cellulose, Sigma-Aldrich, St Louis, Missouri) to mice 5 days per week starting at 6 months of age. Mice, handled daily, were closely monitored for changes and general health resulting from gavage procedures with body mass and mortality recorded throughout the study.

Cytokine Analysis. Cytokine levels were assayed in serum and striatal extracts obtained from rotenone treated mice or vehicle controls using multiplex bead technology (Luminex, Austin, Texas). Cytokine Analysis was performed by Dartlab; Geisel School of Medicine at Dartmouth's Shared Resource for Immunoassays and Flow Cytometry. Assays were performed using a commercially available 32-analyte mouse multiplex kit (Millipore, Darmstadt, Germany).

Immunohistochemistry and Stereology. Tissues were dissected and hemispheres were either submitted for sectioning and tyrosine hydroxylase staining using the Multibrain platform (Neuroscience Associates, Knoxville, Tennessee) or paraffin embedded for thin section immunohistochemical studies performed in house using an automated staining system (Leica Bond Max, Buffalo Grove, Illionois). For stereology, sections were cut at 60 μm and a series of every fourth section (240 μm intervals) was immunohistochemically stained for tyrosine hydroxylase using overnight incubation with Pelfreeze P40101 antibody, (lot 14534, dilution 1:6000), secondary antibody (Vector; goat antirabbit BA1000, lot Y0309, dilution 1:240), and thionine counterstain. Following delineation of the substantia nigra cell counting was conducted using the Optical Fractionator Method (Stereo Investigator, Microbrightfield, Williston, Vermont). For evaluation of microglia, sections of the remaining hemisphere were cut at 5μm and labeled using anti-Iba1 (Novus Biologicals, Littleton, Colorado) and counterstained with hematoxylin. Microglial morphology was scored by a blinded observer in randomly selected fields throughout the mesencephalon using computer-assisted planimetry (Stereo Investigator, Microbrightfield, Williston, Vermont).

Establishment of Primary Mixed Glial Cultures and In Vitro *Toxin Exposure*. Primary cultures containing astroglia and microglia were established from postnatal mice of either the wild type, *Nlrp3*$^{-/-}$, or *IL1R*$^{-/-}$ genetic background. Cultures were expanded for 7 days and enriched for microglia as previously described (Sedgwick *et al.*, 1991). Purified cultures were generated using either fluorescence activated cell sorting (FACS) based on the expression of CD11b (eBioscience, San Diego, California) or using the "shake-off" method (Sedgwick *et al.*, 1991) followed by validation using flow cytometry with the same marker.

SDS-PAGE, ELISA, and QT-PCR Assays. SDS-PAGE was performed using 4%–12% Bis-Tris precast gels (NuPage, ThermoFisher Scientific, Waltham, Massachusetts) subsequently transferred to PVDF membranes. Immunoblots were probed using anti-Nlrp3 (Adipogen, San Diego, California) and anti-Caspase1 (generously provided by Dr Gabriel Nunez, University of Michigan) followed by species-specific HRP-conjugated secondary antibodies (Life Technologies, Grand Island, New York). Cxcl1 and IL1b ELISA assays were performed using the commercially available Quantikine platform (R&D Systems, Minneapolis, Minnesota). QT-PCR assays were performed using SYBR green reagent, primers were designed using NCBI Primer designing tool (www.ncbi.nlm.nih.gov/tools/primer-blast/), sequences available upon request.

Behavioral Analysis. Behavioral analysis in each cohort was evaluated longitudinally with baseline measurements being made immediately prior to the exposure period and repeated measures made at 2-month intervals. Open field studies were conducted using a computer assisted photobeam detection system (TruScan, ThermoFisher Scientific, Waltham, Massachusetts). Animal activity was recorded in 15-min sessions.

RESULTS

Systemic exposure models have the potential to impact multiple systems and *Nlrp3* has a well-characterized role in the peripheral immune system (Schroder and Tschopp, 2010). To identify systemic inflammatory changes resulting from rotenone ingestion, we monitored serum cytokines at regular intervals throughout a 6-month time period during which wild type and *Nlrp3*$^{-/-}$ mice were exposed to low doses of intragastric rotenone 5 days per week. Among the 32 cytokines included in the assay, we consistently detected 18 individual cytokines within the assay range. We normalized these data and conducted longitudinal analysis of the entire data set. We did not identify global changes in the circulating cytokine profile resulting from either genotype or treatment over the exposure period indicating that ingestion of rotenone did not result in broad progressive changes in serum cytokine levels (data not shown). We next evaluated individual cytokines in the normalized data set and identified eotaxin, Cxcl1, IL1a, IL15, G-CSF, IP10, and MCP-1 as having significantly altered levels in at least one time point analyzed (data not shown). With these leads in hand, we returned to the raw data and evaluated each cytokine from this list using longitudinal approaches. We identified a progressive reduction in eotaxin levels resulting from rotenone exposure in wild type mice as compared with mice ingesting vehicle alone (Figure 1A). In mice lacking *Nlrp3*, we noted an initial reduction in eotaxin levels in mice ingesting rotenone, but levels did not continue to decline, rather, levels trended upwards and were highly variable throughout the remainder of the exposure period (Figure 1A). In addition to longitudinal analysis, we tested raw data from individual cytokines corrected for repeated measures at each individual time point. This analysis revealed an *Nlrp3*-dependent increase in Cxcl1 levels in mice ingesting rotenone at 3 months following the initiation of rotenone exposure (Figure 1B). To determine if changes in cytokine levels were associated with cytologic alterations, we collected blood samples from individual wild type and *Nlrp3*$^{-/-}$ mice exposed to rotenone at the time of death and conducted a complete blood count (CBC) using measures analogous to those employed in patient CBCs. Using this technique, we identified an elevated white blood cell (WBC) count (Figure 1C) driven by elevated numbers of circulating lymphocytes (Figure 1D) and neutrophils (Figure 1E) in wild type mice exposed to rotenone not identified in vehicle treated wild type mice or *Nlrp3*$^{-/-}$ mice in either treatment group. These hematologic studies provide strong evidence that *Nlrp3* has a role in mediating alterations in circulating levels of the chemokines eotaxin and Cxcl1 in mice systemically exposed to rotenone in association with alterations in subsets of circulating WBCs.

Following the exposure period, we analyzed brain tissues to characterize neuroinflammatory changes resulting from intragastric rotenone exposure and identify aspects of toxin-induced neuroinflammation that were dependent on *Nlrp3*. We analyzed inflammatory cytokines in striatal extracts, again using the 32-analyte multiplex approach. Analyzing standardized data from this screen we found no significant changes when comparing 1-year-old wild type and *Nlrp3*$^{-/-}$ mice ingesting vehicle for 6 months (data not shown). We observed significant global changes in the cytokine profile in wild type mice ingesting rotenone relative to vehicle treated wild type mice (Figure 2A). This enhanced profile was characterized by increases in multiple cytokines in striatal tissue extracts obtained from wild type rotenone exposed mice compared with mice ingesting vehicle including IL6, Cxcl1, IFNg, IL7, IL15, M-CSF, and VEGF (Figure 2A, denoted by asterisk). When comparing *Nlrp3*$^{-/-}$ mice exposed to rotenone with vehicle controls, we observed reductions in levels of IL1b and IL13 in *Nlrp3*$^{-/-}$ mice that had been exposed to rotenone as compared with mice exposed to vehicle alone (Figure 2B). We further analyzed striatal extracts using SDS-PAGE studies and found that Nlrp3 protein expression was enhanced in mice exposed to rotenone as compared with vehicle alone (Figure 2C). To determine inflammasome activity, we analyzed the inflammasome effector Casp1 in striatal extracts obtained from wild type and *Nlrp3*$^{-/-}$ mice using SDS-PAGE. In these studies, we compared brain extracts obtained from mice lacking *Casp1* in order to identify authentic Casp1 immunoreactive bands. Using this approach, we clearly identified robust induction of the 45kD Casp1 zymogen in both wild type and *Nlrp3*$^{-/-}$ mice treated with rotenone as compared with vehicle treated mice (Figure 2D, 45 kD). In wild type mice treated with rotenone we observed cleavage of Casp1 consistent with inflammasome activity (Figure 2D, 20 kD). In *Nlrp3*$^{-/-}$ mice exposed to rotenone, we observed an increase in levels of the inactive 45 kD Casp1 zymogen at the expense of the 20kD, activated form of the enzyme. These findings are consistent with enhanced activity of the inflammasome in mice ingesting rotenone and indicated that *Nlrp3* had a critical role in rotenone-induced neuroinflammation.

Seeking further evidence of rotenone-induced neuroinflammation we analyzed microglia using immunohistochemical techniques in histologic sections obtained from the brains of wild type and *Nlrp3*$^{-/-}$ mice that had been exposed to rotenone for 6 months. Staining for the microglia specific marker Iba1, we defined microglial activity based on cellular morphology; resting or ramified microglia characterized by numerous thin cellular processes (Figure 3A), intermediate “bushy” microglia identified as having thicker less numerous processes (Figure 3B), and activated microglia having an amoeboid morphology (Figure 3C) (Kreutzberg, 1996). In vehicle treated wild type mice, we observed that the majority of mesencephalic microglia were in the resting state and we detected very few activated microglia (Figure 3D). In wild type mice exposed to rotenone, we found a significant increase in the numbers of activated microglia at the expense of those in the resting state, consistent with the reports of others indicating that systemic exposure to

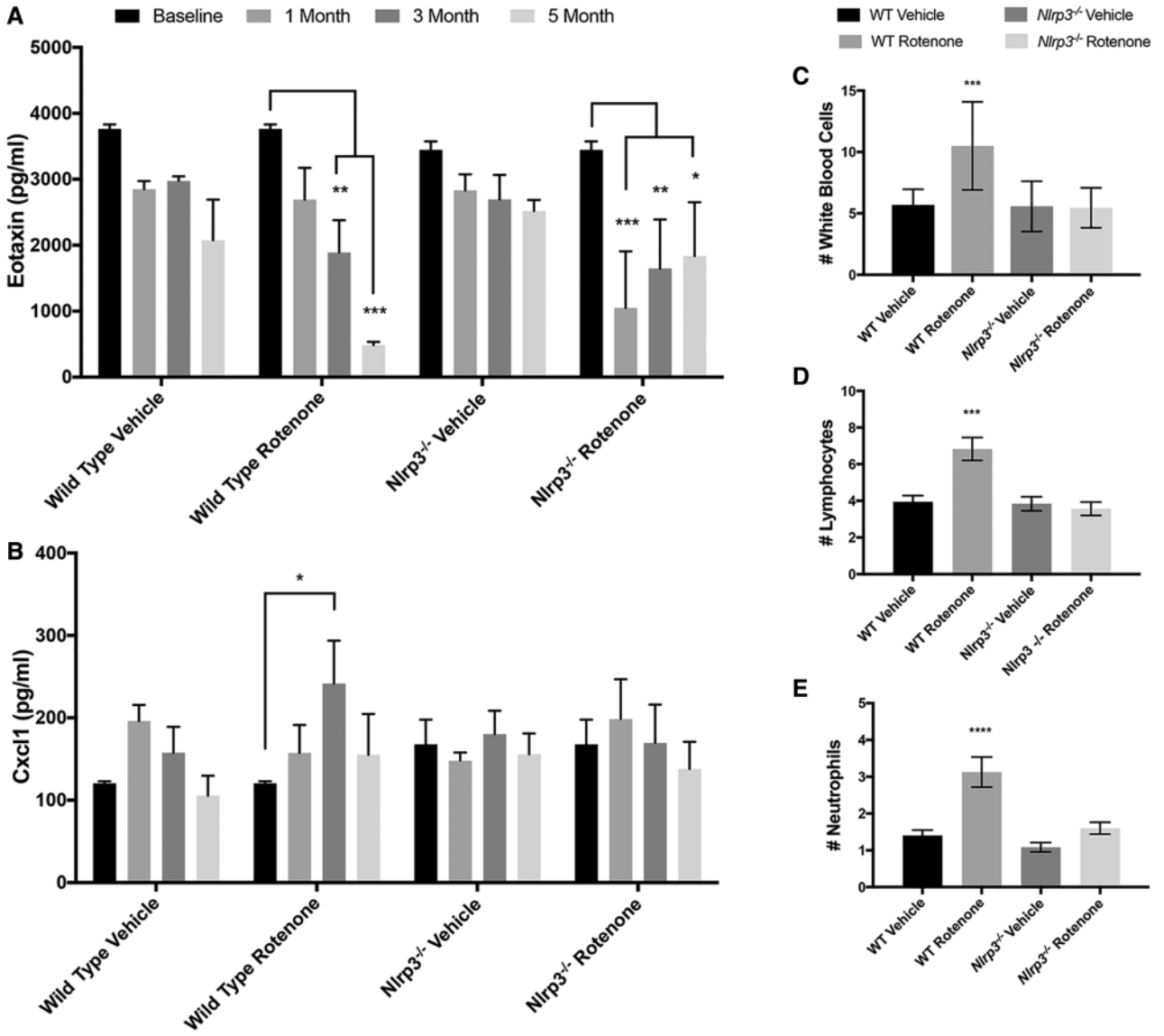

Figure 1. Longitudinal multiplex cytokine analysis of wild type and *Nlrp3*$^{-/-}$ mice exposed to rotenone. Serum samples from mice were obtained using tail bleeds at baseline and bimonthly intervals throughout the exposure period. Samples from individual animals were pooled into 3 groups per treatment/genotype (n = 3) and analyzed using the Luminex platform. A, A significant interaction between genotype and time was detected in eotaxin levels reflecting a progressive decline in eotaxin in wild type mice exposed to rotenone (2-way RM ANOVA, p value = .036, Dunnet's Multiple Comparison Test, p value * < .05, **p value < .001, ***p value < .0001). B. Multiple comparison analysis detected elevated levels of Cxcl1 in wild type mice exposed to rotenone following 3 months of exposure not detected in *Nlrp3*$^{-/-}$ mice (Dunnet's Multiple Comparison Test, p value * < .05). C–E, Whole blood was collected from mice following 6 months of rotenone exposure into EDTA spray coated collection tubes using tail bleeds. Blood samples were analyzed using a veterinary hematology analyzer per manufacturer's instructions. Significant *Nlrp3*-depedent elevations were detected in the numbers of total WBCs (C), lymphocytes (D), and neutrophils (E) in wild type mice ingesting rotenone (***p value < .001, ****p value < .0001, Ordinary 1-way ANOVA).

rotenone activated microglia in the rat central nervous system (CNS) (Sherer *et al.*, 2003). Similar analysis of *Nlrp3*$^{-/-}$ mice revealed the presence of increased numbers of microglia with a less differentiated amoeboid morphology in both vehicle and rotenone treated groups, although these changes were neither dependent on exposure to rotenone nor were they statistically significant (Figure 3E). Taken together, findings of a significant degree of *Nlrp3*-dependent microglial activation resulting from long-term low dose rotenone exposure in mice further substantiates the role of *Nlrp3* in mediating rotenone-induced neuroinflammatory changes.

Previous reports by others document significant nigral cell loss resulting from intragastric exposure to rotenone in mice (Inden *et al.*, 2011; Pan-Montojo *et al.*, 2010). We conducted unbiased stereologic cell counts to determine if loss of *Nlrp3* resulted in increased sparing of nigral neurons in mice exposed to rotenone. We specifically analyzed neurons of the SNpC and consistent with previous reports found reductions in neuron number and density in wild type mice exposed to 5 mg/kg oral rotenone for 6 months as compared with vehicle treated mice (Figs. 4A, B, E, F, I, and J) (Pan-Montojo *et al.*, 2010). We found SNpC cell numbers to be normal in *Nlrp3*$^{-/-}$ mice treated with vehicle, and did not identify any cell loss in *Nlrp3*$^{-/-}$ mice exposed to rotenone (Figs. 4C, D, F–H, and I). Our analysis of *Nlrp3*$^{-/-}$ mice exposed to rotenone provides evidence of the suitability of these mice for toxicologic studies that require

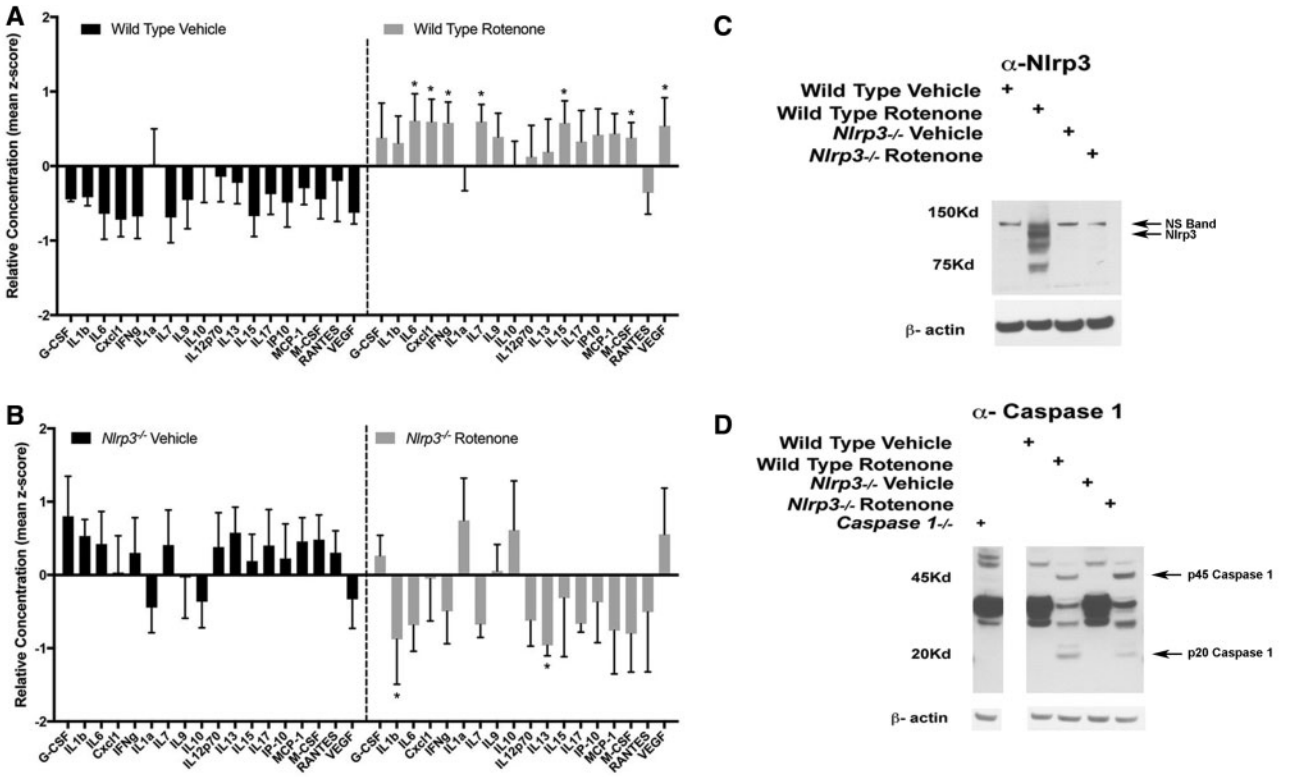

Figure 2. Analysis of inflammatory mediators in striatal extracts obtained from wild type and Nlrp3$^{-/-}$ mice exposed to rotenone. A and B, Freshly dissected striatal tissues were obtained from wild type and *Nlrp3*$^{-/-}$ mice exposed to either vehicle and rotenone following 6 months of exposure and homogenized for inflammatory cytokine analysis. Extracts were analyzed in triplicate using a 32-plex multiple cytokine bead based assay. Z-scored data were analyzed for global changes, significant overall treatment effects were observed when comparing the inflammatory cytokine signature of rotenone treated wild type animals to vehicle treated groups at each time point (p value $< .001$, 2-way ANOVA, n = 4 per group). Asterisks indicate individual cytokines identified using this screen as having significantly altered levels as compared with vehicle controls (Dunnet's Multiple Comparison Test, p value* $< .05$). C and D, Representative immunoblots generated following SDS-PAGE analysis of striatal extracts obtained from treatment groups described above indicating elevated Nlrp3 expression and caspase 1 cleavage in wild type mice exposed to rotenone (n = 4 per group).

animals to survive to advanced ages. Our studies also provide an important extension of a report indicating that loss of *Nlrp3* protects mice from SNpC degeneration as observed in the MPTP acute toxicity model (Yan *et al.*, 2015) by demonstrating for the first time that *Nlrp3* is required for nigral degeneration in a chronic intragastric pesticide exposure model of PD.

We observed changes in levels of the chemokine Cxcl1 in both serum (Figure 1B) and brain tissues (Figure 2A) along with elevated numbers of circulating neutrophils (Figure 1E), a key target of Cxcl1 (Kolaczkowska and Kubes, 2013). To explore our finding of elevated Cxcl1 in brain tissues obtained from mice exposed to rotenone, and identify a cellular origin for Cxcl1 in the CNS, we established primary mixed glial cultures containing both astrocytes and microglia from postnatal mice. We treated wild type cultures with rotenone alone or rotenone following LPS priming and identified a robust rotenone-dependent induction of *Cxcl1* mRNA in mixed glial cultures primed with LPS using QT-PCR (Figure 5A). We extended these studies to evaluate *IL1b* transcript, a key downstream indicator of inflammasome activity, and observed significant elevation of *IL1b* transcript in mixed glial cultures primed with LPS and then treated with rotenone (Figure 5B), consistent with previous reports (Gustin *et al.*, 2015). To dissect the cellular origins of *Cxcl1* and *IL1b* in these cultures that contained both astrocytes and microglia, we treated wild type mixed glial cultures as above and sorted using FACS based on expression of the microglia-specific marker CD11b (Figure 5C). We found that *Cxcl1* expression was enriched in the CD11b negative astroglial population (Figure 5D) while *IL1b* was enriched in the CD11b-positive microglia (Figure 5E). This finding was consistent with previous reports characterizing rotenone-mediated microglial *IL1b* expression (Sarkar *et al.*, 2015) and prompted us to evaluate whether astroglial *Cxcl1* resulted from an interaction between microglia and astroglia.

We observed rotenone-mediated induction of the *Cxcl1* transcript in wild type astrocytes in association with microglial *IL1b* expression (Figs. 5D and E) suggesting that a previously reported microglial *Nlrp3-IL1b* axis (Gustin *et al.*, 2015; Sarkar *et al.*, 2015) may be operative in our co-culture system. To analyze more specifically the role of *Nlrp3*, we used ELISA to analyze Cxcl1 secretion in mixed glial cultures obtained from wild type and *Nlrp3*$^{-/-}$ mice. We observed robust secretion of Cxcl1 in LPS primed cultures treated with rotenone but did not observe significant Cxcl1 release in *Nlrp3*$^{-/-}$ cultures (Figure 6A). Since *Nlrp3* was required for robust induction of *Cxcl1* expression by rotenone in primed co-cultures, we worked to confirm our sorting results suggesting that microglia were the source of *Nlrp3* activity in mixed cultures (Figure 5E). Using well-characterized techniques to remove microglia we establish purified astrocyte cultures and found that while astroglia could be induced to secrete Cxcl1, the removal of microglia significantly reduced the secretion of Cxcl1 as compared with that observed in mixed cultures (Figure 6B). Based on previous studies (Sarkar *et al.*, 2015; Shaftel *et al.*, 2007), we reasoned that microglial IL1b might be

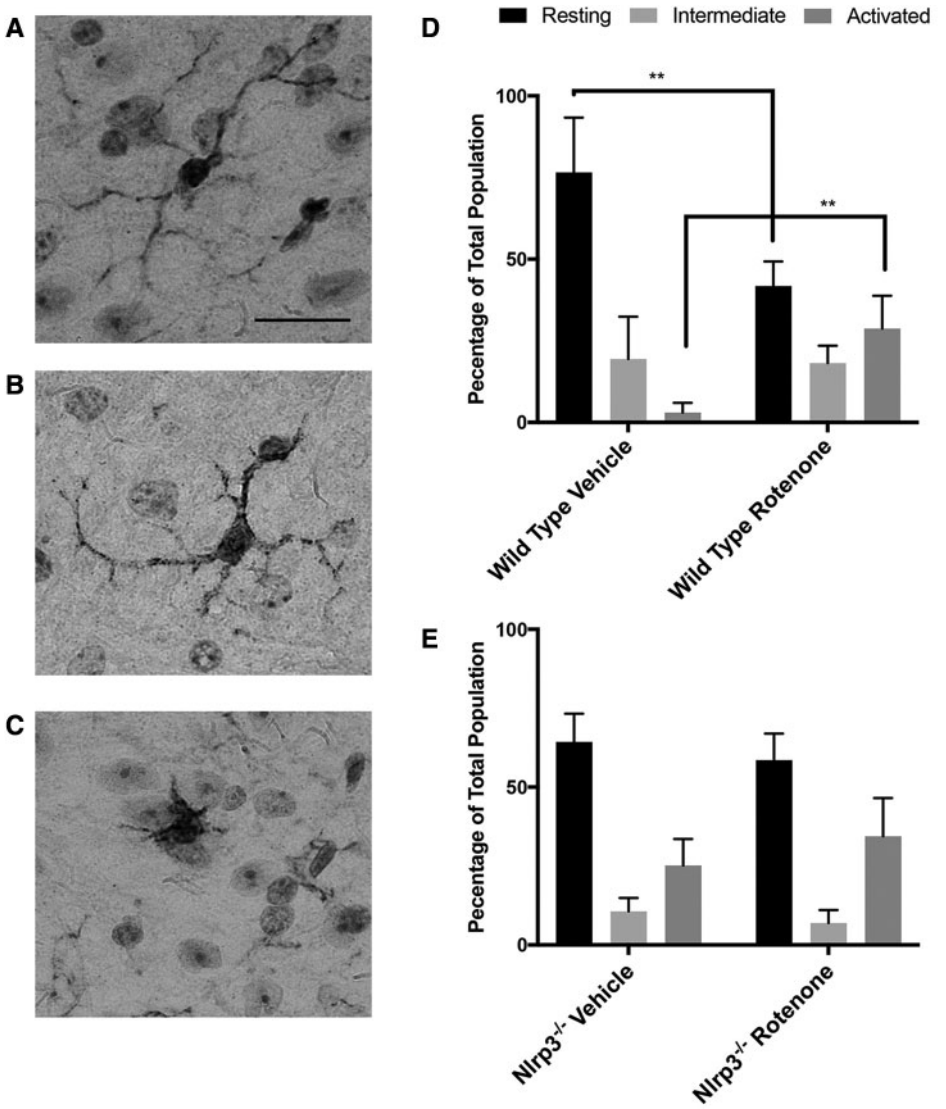

Figure 3. Analysis of microglial morphology in histologic sections obtained from wild type and Nlrp3$^{-/-}$ mice exposed to rotenone. Histologic sections were prepared from wild type and *Nlrp3*$^{-/-}$ mice exposed to rotenone or vehicle alone and immunostained using antiIba1 antibody. The entire mesencephalon was delineated and microglia were counted using computer-assisted planimetry. Iba1-positive microglial morphology was defined as follows: Resting or ramified microglia characterized by numerous thin cellular processes (A), intermediate "bushy" microglia identified as having thicker less numerous processes (B), and activated microglia having an amoeboid morphology (C). Percentages of microglia of each morphology were determined in wild type (D) and *Nlrp3*$^{-/-}$ (E) mice. A significant reduction in the number of microglia of activated morphology were detected in wild type mice exposed to rotenone compared with vehicle at the expense of microglia of the resting morphology (**p value $< .01$, Ordinary 1-way ANOVA with Dunnet's Multiple Comparison Test).

important in induction of Cxcl1 in astrocytes. We found that the primary receptor for IL1b, interleukin 1 receptor (IL1R), was expressed in purified astrocytes and that rotenone was able to significantly elevate the expression of astroglial *IL1R* in LPS-primed cultures (Figure 6C). We compared the ability of LPS and rotenone to induce Cxcl1 release in wild type and *IL1R*$^{-/-}$ mixed glial cultures and found that rotenone was able to significantly enhance Cxcl1 secretion in wild type cultures but that this induction was lost in cultures isolated from mice lacking *IL1R* (Figure 6D). Taken together our findings support a model consistent with previous reports indicating activity of the Nlrp3-inflammasome in primary microglia (Gustin *et al.*, 2015; Halle *et al.*, 2008; Sarkar *et al.*, 2015; Shaftel *et al.*, 2007). In addition, we identify astrocytes as a cellular origin of the *Nlrp3*-dependent induction of Cxcl1, a chemokine whose elevation is observable in serum and CNS tissues obtained from mice ingesting rotenone.

DISCUSSION

Characterizing genes required for neurodegeneration resulting from systemic toxin exposure is of broad interest towards improving the understanding of age-related neurologic disorders with environmental components, such as PD (Cannon and Greenamyre 2011, 2013). Here, we expose wild type and *Nlrp3*$^{-/-}$ mice to low doses of rotenone over an extended time course. Over this time, mice develop progressive *Nlrp3*-dependent serologic abnormalities in association with neuroinflammatory changes and nigral cell loss observed in postmortem brain tissues. In vitro studies support a model by which microglia and astrocytes interact to generate *Nlrp3*-dependent Cxcl1, a diffusible chemokine that we observe systemically in mice exposed to rotenone. These data confirm and expand upon the initial report of this protocol (Pan-Montojo *et al.*, 2010) and indicate that

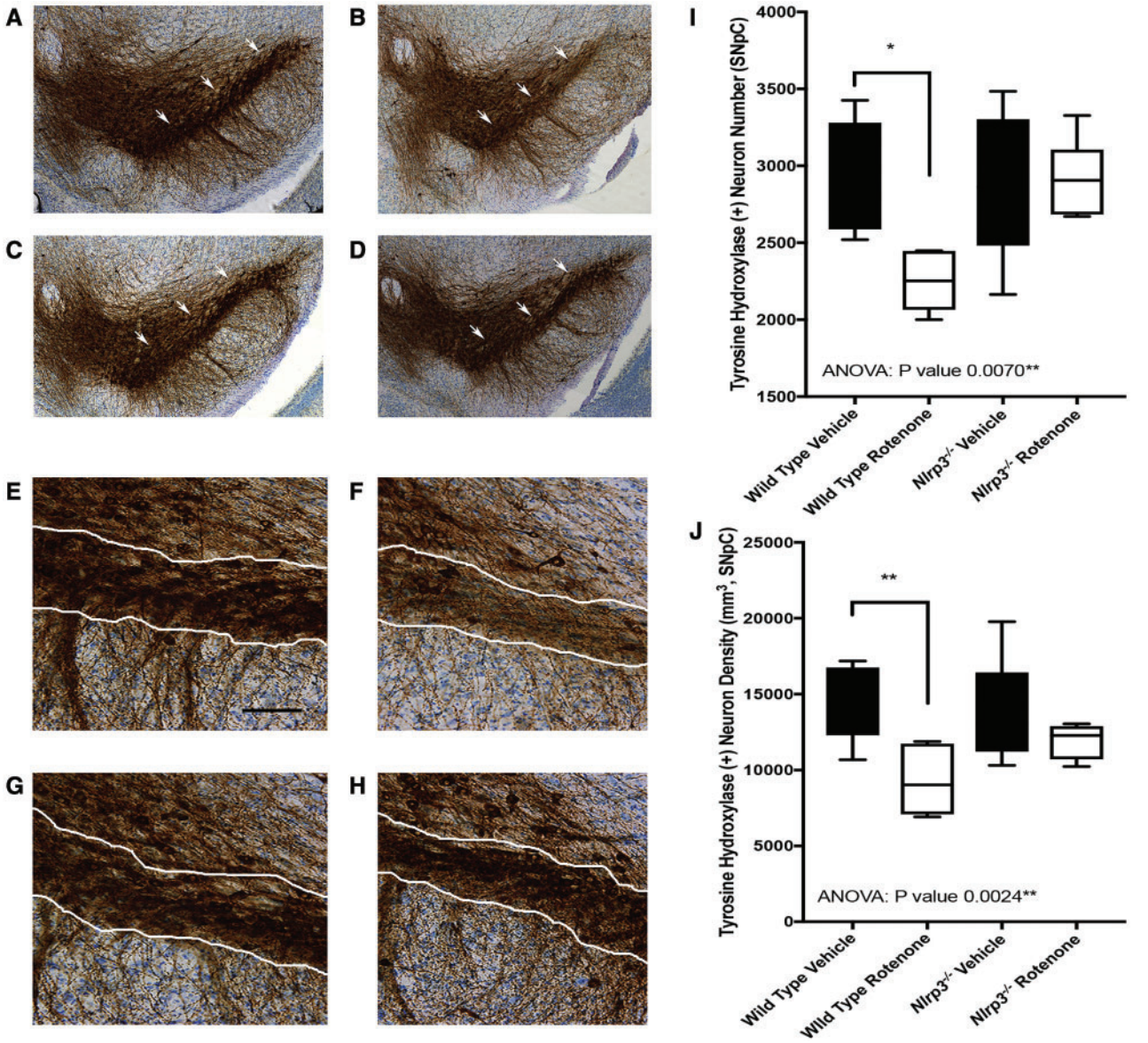

Figure 4. Stereologic analysis of SNpc neurons in histologic sections obtained from wild type and Nlrp3$^{-/-}$ mice exposed to rotenone. 60 μM histologic sections were prepared from single hemispheres and stained for tyrosine hydroxylase by Neuroscience Associates (Knoxville, Tennessee). Stereologic cell counts were conducted using the Stereo Investigator platform (Microbrightfield, Williston, Vermont). Representative photomicrographs constructed from multiple images (original magnification 20×) showing the SNpC (white arrows) in wild type mice exposed to vehicle (A), wild type mice exposed to rotenone (B), *Nlrp3*$^{-/-}$ mice exposed to vehicle (C), and *Nlrp3*$^{-/-}$ mice exposed to rotenone (D). Representative photomicrographs (original magnification 20×, scale bar represents 75 μM) showing the SNpC (white bordered region) in wild type mice exposed to vehicle (E), wild type mice exposed to rotenone (F), *Nlrp3*$^{-/-}$ mice exposed to vehicle (G), and *Nlrp3*$^{-/-}$ mice exposed to rotenone (H). Stereologic quantitation indicates a significant *Nlrp3*-dependent reduction in the number (I) and density (J) of tyrosine hydroxylase-positive SNpc neurons in wild type mice exposed to rotenone (n = 8 per group, p value = .0070 Ordinary 1-way ANOVA, *p value < .05, **p value < .01, Dunnet's Multiple Comparison Test).

long-term intragastric exposure to low doses of rotenone is an appropriate model to evaluate prodromal inflammation associated with the development of parkinsonism. Equally important, these results add to a growing database indicating that *Nlrp3* is required for nigral cell loss in animal models of PD (Qiao *et al.*, 2016; Yan *et al.*, 2015) and indicate that *Nlrp3* may have a broad role in mediating toxin-induced systemic and neurologic inflammation.

Our data provide evidence of rotenone-mediated microglial activation (Figure 3) consistent with observations made in postmortem tissues from PD patients (McGeer *et al.*, 1988) and numerous previous reports in animal models of PD (Czlonkowska *et al.*, 1996; McGeer *et al.*, 2003; Sherer *et al.*, 2003). We did not observe rotenone-mediated changes in microglia in *Nlrp3*$^{-/-}$ mice indicating that *Nlrp3* was required for rotenone-induced microglial activation. Interestingly, we did observe a genotype-dependent alteration in microglial morphology in *Nlrp3*$^{-/-}$ mice typified by a reduction in cellular processes (Figure 3E). This phenotypic alteration is previously unreported in mice, however, similar alterations in microglial morphology have been observed in zebrafish harboring a mutation in the NOD-like receptor *nlrc3-like* (Shiau *et al.*, 2013). In this report, authors ascribe the defect to deregulated microglial development and maturation. We cannot infer the origins of the changes we observe in microglial phenotype using our histologic data; however, we are keen to comprehensively analyze microglia in *Nlrp3*$^{-/-}$ mice

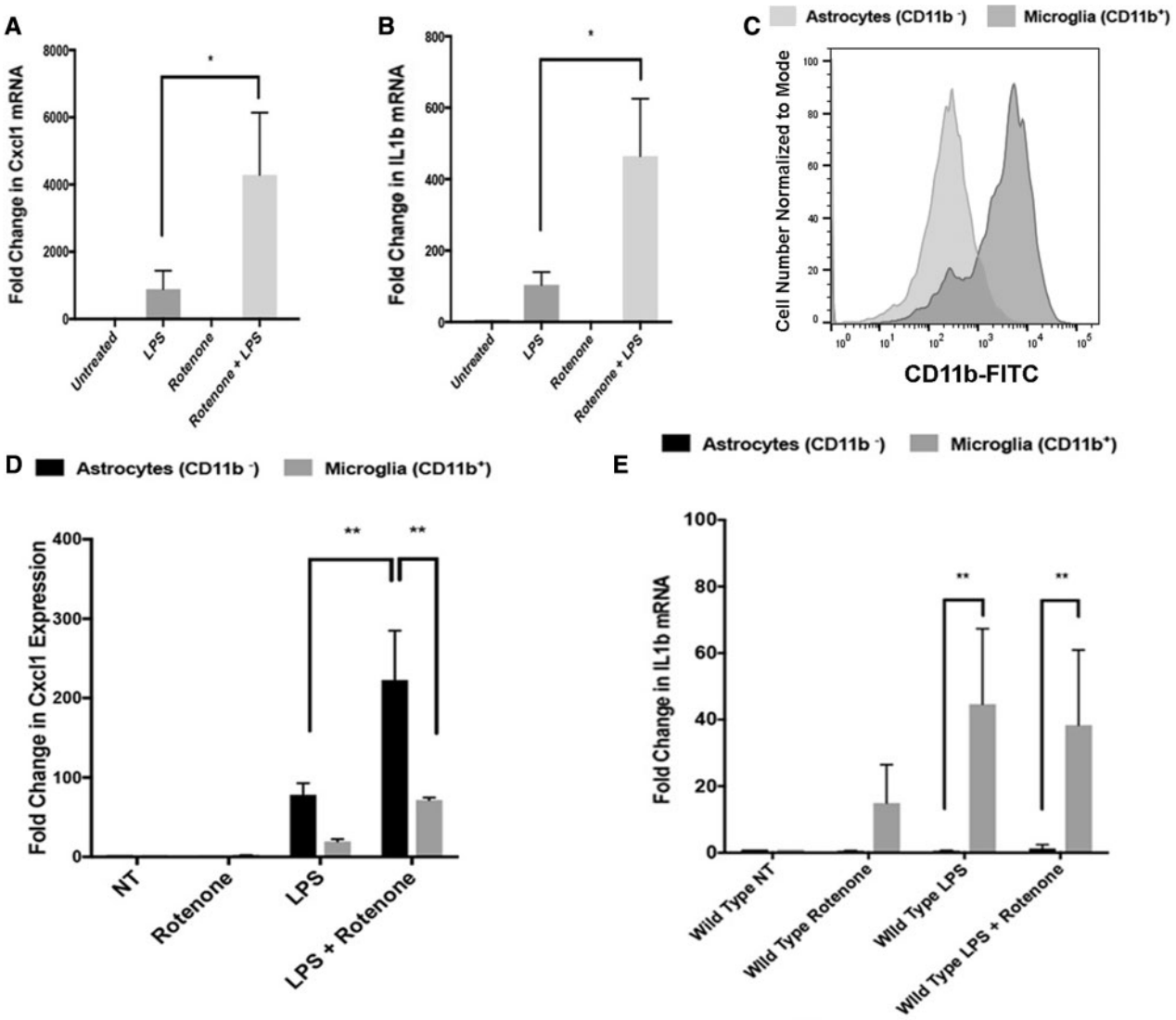

Figure 5. Astrocytes are a cellular origin of rotenone-induced Cxcl1. Total mRNA was collected from primary mixed glial cultures reverse transcribed and analyzed using Real-Time PCR. Rotenone treatment significantly elevated *Cxcl1* (A) and *IL1b* (B) mRNA levels as compared with LPS treatment alone (Representative experiment conducted in triplicate, n = 3 per group, **p* value < .05 Ordinary 1-way ANOVA with Dunnet's Multiple Comparison Test). C, Mixed glial cultures were separated using the shake off method and separation of microglia from astrocytes was confirmed by flow cytometry anti-CD11b-FITC antibodies. The expression of *Cxcl1* and *IL1B* mRNA was assayed in purified astrocytes and microglia using Real-Time PCR. Rotenone treatment significantly elevated *Cxcl1* (D) and *IL1b* (E) mRNA levels as compared with LPS treatment alone. A significant majority of Cxcl1 expression was detected in CD11b-negative astrocytes (D) while a significant majority of *IL1b* (E) expression was detected in CD11b-positive microglia (Representative experiment conducted in triplicate, n = 3 per group, ***p* value < .01 Ordinary 1-way ANOVA with Dunnet's Multiple Comparison Test).

towards understanding both their development and how *Nlrp3* loss impacts the spectrum of classical and nonclassical activation phenotypes observed throughout normal aging and following inflammatory insult (Grabert *et al.*, 2016).

A role for Cxcl1 in PD has not been extensively described, however, a recent study found that alterations in Cxcl1 protein levels were a core component of a discriminatory multi-protein cytokine panel capable of differentiating PD from PD with dementia (Lue *et al.*, 2016). Persistent Cxcl1 elevation has also been observed in MPTP treated mice (Parillaud *et al.*, 2017) and implicated in dopaminergic differentiation in rats (Edman *et al.*, 2008). Our *in vitro* findings support a model in which astroglial Cxcl1 is induced by a microglial Nlrp3/IL1b-dependent mechanism. Cxcl1 expression has been previously reported in the CNS downstream of IL1b where its expression is associated with neutrophil infiltration (Shaftel *et al.*, 2007). CNS IL1b also induces hepatic Cxcl1 that has been associated with leukocyte recruitment into the brain in injury models (Campbell *et al.*, 2005). Although we observed a strong induction of IL1b and a requirement of *IL1R* for Cxcl1 induction in vitro (Figs. 5 and 6), we only observed low levels of IL1b in brain extracts where we saw a trend towards elevated IL1b in extracts obtained from wild type mice exposed to rotenone (Figure 2). Although our cytokine screening data did not identify significant changes in IL1b, we did note that only wild type mice treated with rotenone demonstrated detectable levels of IL1b with high penetrance, in line with our findings in mixed glial cultures (Figure 5).

Neutrophils are well-characterized mediators of acute and chronic inflammation (Deniset and Kubes, 2016; Soehnlein *et al.*, 2017) and contribute to oxidative stress associated with PD

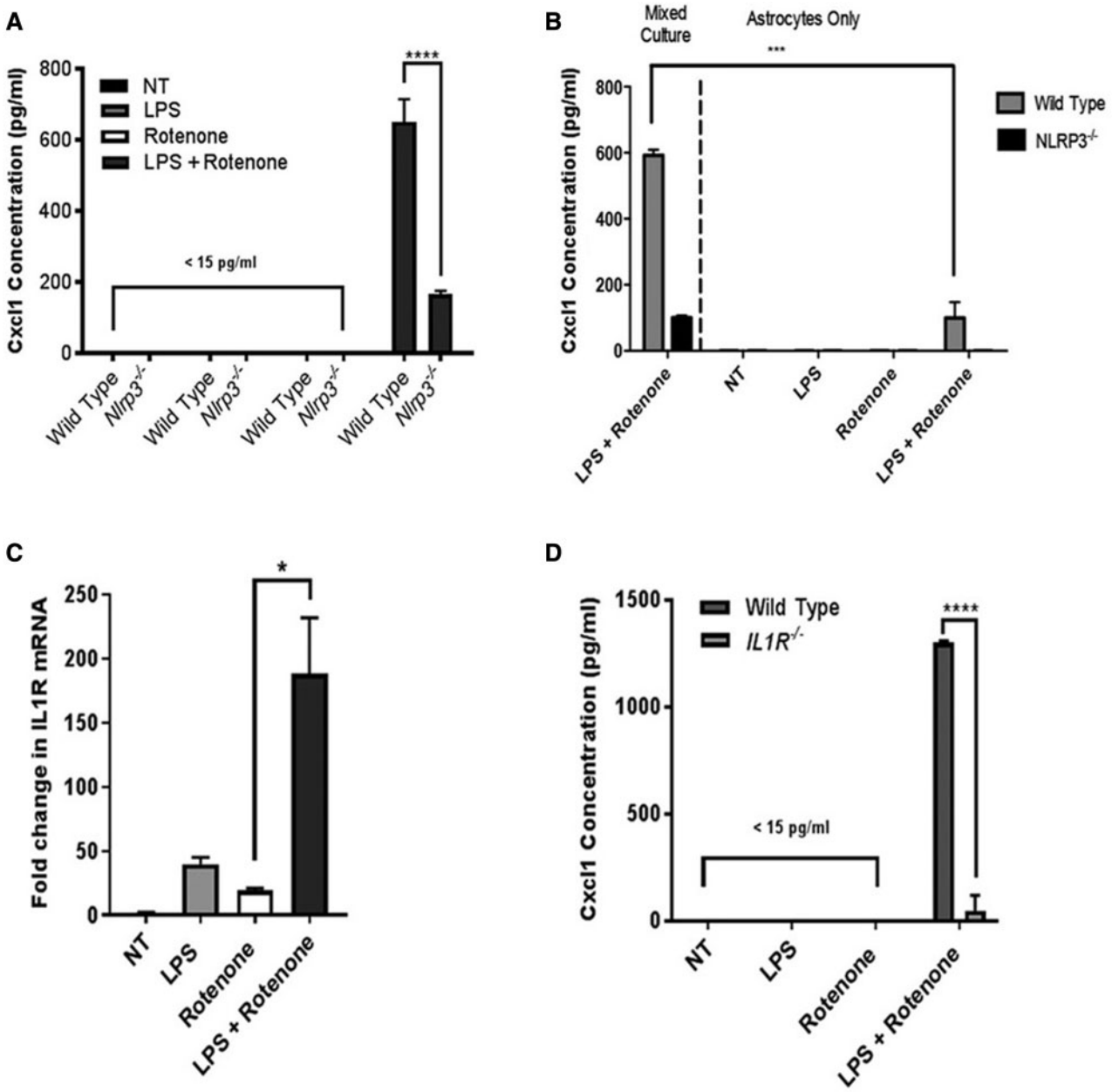

Figure 6. Microglia are required for normal levels of Nlrp3-dependent Cxcl1 secretion resulting from rotenone exposure. Primary mixed glia or astrocytes alone derived from wild type and *Nlrp3*$^{-/-}$ mice were exposed to rotenone and/or the priming agent LPS. A, Treated mixed glial cultures were assayed for Cxcl1 secretion using ELISA. Robust *Nlrp3*-depedent induction of Cxcl1 secretion was observed in primed cultures treated with rotenone. B, Treated astrocyte alone cultures were assayed for Cxcl1 secretion using ELISA and compared with mixed glial cultures. Cxcl1 secretion levels were significantly reduced in astrocyte alone cultures as compared with similarly treated mixed cultures. C, Total mRNA was collected from astrocyte alone cultures, reverse transcribed, and analyzed for expression of *IL1R* using Real-Time PCR. Rotenone treatment significantly elevated *IL1R* expression in LPS primed cultures. D, Treated mixed glial cultures obtained from wild type or *IL1R*$^{-/-}$ mice were assayed for Cxcl1 secretion using ELISA. Robust *IL1R*-depedent induction of Cxcl1 secretion was observed in primed cultures treated with rotenone. (A–D) Representative experiments conducted in triplicate, n = 3 per group, $^{*}p$ value < .05 $^{***}p$ value < .001, $^{****}p$ value < .0001, Ordinary 1-way ANOVA with Dunnet's Multiple Comparison Test.

(Gatto *et al.*, 1996). Cxcl1 is a key chemoattractant important in the elaboration and recruitment of neutrophils into tissues (Kolaczkowska and Kubes, 2013). We examined closely brain tissues obtained from mice ingesting rotenone and found no evidence of neutrophil recruitment into the CNS (data not shown) in spite of our observation of elevated numbers of circulating neutrophils (Figure 1). Close inspection of immunostained tissues obtained from rotenone treated mice revealed an obvious GFAP-positive perivascular cuff, consistent with the role of astrocytes in regulating the permeability of the blood brain barrier (BBB) (Supplementary Figure 1). Although our studies cannot rule out other sources of Cxcl1, our findings suggest that we have captured a snapshot in the progression of PD symptomology at which time systemic and CNS inflammatory activity and nigral cell loss is apparent, but prior to peripheral immune cell infiltration; possibly held at bay by astroglial barrier formation at the BBB (Sofroniew, 2009; Sofroniew and Vinters, 2010). Our finding that astroglia reside at the BBB interface (Supplementary Figure 1) and

secrete significant amounts of Cxcl1 in response to rotenone (Figs. 6 and 7) suggests a model by which the brain may influence peripheral immune cells. The build-up and spike in circulating Cxcl1 followed by a reduction at late time points coincident with elevated neutrophil numbers (Figure 1) is consistent with depletion of circulating Cxcl1 resulting from mobilization of neutrophil reserves in the bone marrow (Furze and Rankin, 2008). This finding merits further exploration in the context of biomarker identification and highlights the utility of the chronic rotenone model for making new discoveries related to PD progression.

Numerous toxin-based rodent models of PD have been developed that vary in their development of motor symptoms (Tieu, 2011). To our knowledge no studies have evaluated motor behaviors in aging *Nlrp3*$^{-/-}$ mice. In our study, we observed a decrease in baseline spontaneous activity and a more rapid decline throughout aging in *Nlrp3*$^{-/-}$ mice compared with wild type mice not related to rotenone exposure (Supplementary Figure 2). Our study design does not address the mechanism for this deficiency, however, based on our serologic and histologic studies, we know that this finding is associated with deregulated cytokine levels (Figs. 1 and 2) and unexplained alterations in microglial morphology (Figure 3) that are also unrelated to rotenone exposure. These observations add to a growing database that has implicated the immune mediator *Nlrp3* in behavioral abnormalities, including chronic fatigue syndrome (Zhang *et al.*, 2016) and anxiety-like behaviors (Xu *et al.*, 2016). Findings suggest that *Nlrp3* may have a role in maintaining homeostasis in multiple tissues and indicate that further studies to determine the role of *Nlrp3* during normal aging and disease are of interest.

In our unbiased and longitudinal cytokine assays, we detected a progressive decline in C-C motif chemokine eotaxin (a.k.a. CCL11) in wild type mice ingesting rotenone. Eotaxin is best characterized in airway inflammatory diseases where it is capable of driving the accumulation of eosinophils in the lungs (Pope *et al.*, 2005). Although the role of eotaxin in brain diseases has not been well characterized to date, in cases where it has been measured, levels have typically been reported as increased in association with neurologic disease (Bettcher *et al.*, 2016; Chandra *et al.*, 2016; Wild *et al.*, 2011). We did not detect any changes in circulating eosinophil number in mice ingesting rotenone and inspection of histologic sections of brain tissue stained with hematoxylin and eosin did not reveal any obvious indicators of granulocyte infiltration resulting from genotype or treatment (data not shown). As such, our observation of progressive changes in eotaxin levels may represent a novel serologic indicator of systemic inflammation associated with neurodegeneration and pesticide exposure.

In the study, we have employed a slowly developing mouse model of parkinsonism to identify novel cellular and molecular characteristics of neuroinflammation resulting from exposure to the disease-associated environmental toxin rotenone. The study provides robust longitudinal data identifying systemic and neurologic inflammatory changes resulting from rotenone exposure. In addition, we identify *Nlrp3* as a key mediator of the inflammatory and neurodegenerative processes associated with rotenone intoxication. These findings are important because inflammasome genes like *Nlrp3* may function in a core pathway driving sterile inflammatory processes associated with chemical exposure, proteinopathy, and metabolic stress; all key factors influencing the incidence and progression of PD.

SUPPLEMENTARY DATA

Supplementary data are available at *Toxicological Sciences* online.

ACKNOWLEDGMENTS

We acknowledge the guidance and support provided by Dartlab, Dartmouth's Resource for Immunoassays and Flow Cytometry along with Rebecca O'Meara and the staff at Norris Cotton Cancer Center's Research Pathology Shared Resource. We are grateful for the expert guidance and support in analysis of PD symptomology provided by Dr William Hickey, Dr Stephen Lee, and Dr Mary Feldman of the Department of Neurology at Dartmouth-Hitchcock Medical Center. We thank Dr Gabriel Nunez of the University of Michigan for generously providing key reagents for the study. We are indebted to Dr Mark Israel, Dr Jay Dunlap, Dr Hermes Yeh, Dr Leslie Henderson and Dr Duane Compton of the Geisel School of Medicine at Dartmouth for their mentorship and unwavering support of the research program. We thank Tabatha Richardson for help in the preparation of the manuscript.

FUNDING

This work is supported by the National Institute for Environmental Health Sciences at the National Institutes of Health (NIH) (1R01ES024745-01A1, to M.C.H.) and a Fellowship from the National Institute for Neurological Disorders and Stroke at NIH (Grant number F31 NS 098630 – 01 to E.M.M.).

REFERENCES

Abbas, N., Lucking, C. B., Ricard, S., Durr, A., Bonifati, V., De Michele, G., Bouley, S., Vaughan, J. R., Gasser, T., Marconi, R., on Genetic Susceptibility in Parkinson's Disease., *et al.* (1999). A wide variety of mutations in the parkin gene are responsible for autosomal recessive parkinsonism in Europe. French Parkinson's Disease Genetics Study Group and the European Consortium. *Hum. Mol. Genet.* **8**, 567–574.

Betarbet, R., Sherer, T. B., MacKenzie, G., Garcia-Osuna, M., Panov, A. V., and Greenamyre, J. T. (2000). Chronic systemic pesticide exposure reproduces features of Parkinson's disease. *Nat. Neurosci.* **3**, 1301–1306.

Bettcher, B. M., Fitch, R., Wynn, M. J., Lalli, M. A., Elofson, J., Jastrzab, L., Mitic, L., Miller, Z. A., Rabinovici, G. D., Miller, B. L., *et al.* (2016). MCP-1 and eotaxin-1 selectively and negatively associate with memory in MCI and Alzheimer's disease dementia phenotypes. *Alzheimers Dement (Amst)* **3**, 91–97.

Blesa, J., Phani, S., Jackson-Lewis, V., and Przedborski, S. (2012). Classic and new animal models of Parkinson's disease. *J. Biomed. Biotechnol.* **2012**, 845618.

Campbell, S. J., Perry, V. H., Pitossi, F. J., Butchart, A. G., Chertoff, M., Waters, S., Dempster, R., and Anthony, D. C. (2005). Central nervous system injury triggers hepatic CC and CXC chemokine expression that is associated with leukocyte mobilization and recruitment to both the central nervous system and the liver. *Am. J. Pathol.* **166**, 1487–1497.

Canet, A. R. M., Wilson, M. A., Miller, D. W., Ahmad, R., McLendon, C., Bandyopadhyay, S., Baptista, M. J., Ringe, D., Petsko, G. A., and Cookson, M. R. (2004). The Parkinson's disease protein DJ-1 is neuroprotective due to cysteine-sulfinic acid-driven mitochondrial localization. *Proc. Natl. Acad. Sci. U.S.A.* **101**, 9103–9108.

Cannon, J. R., and Greenamyre, J. T. (2011). The role of environmental exposures in neurodegeneration and neurodegenerative diseases. *Toxicol. Sci.* **124**, 225–250.

Cannon, J. R., and Greenamyre, J. T. (2013). Gene-environment interactions in Parkinson's disease: Specific evidence in humans and mammalian models. *Neurobiol. Dis.* **57**, 38–46.

Cannon, J. R., Tapias, V., Na, H. M., Honick, A. S., Drolet, R. E., and Greenamyre, J. T. (2009). A highly reproducible rotenone model of Parkinson's disease. *Neurobiol. Dis.* **34**, 279–290.

Chandra, G., Rangasamy, S. B., Roy, A., Kordower, J. H., and Pahan, K. (2016). Neutralization of RANTES and eotaxin prevents the loss of dopaminergic neurons in a mouse model of Parkinson disease. *J. Biol. Chem.* **291**, 15267–15281.

Codolo, G., Plotegher, N., Pozzobon, T., Brucale, M., Tessari, I., Bubacco, L., and de Bernard, M. (2013). Triggering of inflammasome by aggregated alpha-synuclein, an inflammatory response in synucleinopathies. *PloS One* **8**, e55375.

Czlonkowska, A., Kohutnicka, M., Kurkowska-Jastrzebska, I., and Czlonkowski, A. (1996). Microglial reaction in MPTP (1-methyl-4-phenyl-1,2,3,6-tetrahydropyridine) induced Parkinson's disease mice model. *Neurodegeneration* **5**, 137–143.

Dardiotis, E., Xiromerisiou, G., Hadjichristodoulou, C., Tsatsakis, A. M., Wilks, M. F., and Hadjigeorgiou, G. M. (2013). The interplay between environmental and genetic factors in Parkinson's disease susceptibility: the evidence for pesticides. *Toxicology* **307**, 17–23.

de Lau, L. M., and Breteler, M. M. (2006). Epidemiology of Parkinson's disease. *Lancet Neurol.* **5**, 525–535.

Deniset, J. F., and Kubes, P. (2016). Recent advances in understanding neutrophils. *F1000Research* **5**, 2912.

Drolet, R. E., Cannon, J. R., Montero, L., and Greenamyre, J. T. (2009). Chronic rotenone exposure reproduces Parkinson's disease gastrointestinal neuropathology. *Neurobiol. Dis.* **36**, 96–102.

Duty, S., and Jenner, P. (2011). Animal models of Parkinson's disease: A source of novel treatments and clues to the cause of the disease. *Br. J. Pharmacol.* **164**, 1357–1391.

Edman, L. C., Mira, H., Erices, A., Malmersjo, S., Andersson, E., Uhlen, P., and Arenas, E. (2008). Alpha-chemokines regulate proliferation, neurogenesis, and dopaminergic differentiation of ventral midbrain precursors and neurospheres. *Stem Cells* **26**, 1891–1900.

Furze, R. C., and Rankin, S. M. (2008). Neutrophil mobilization and clearance in the bone marrow. *Immunology* **125**, 281–288.

Gatto, E. M., Carreras, M. C., Pargament, G. A., Riobo, N. A., Reides, C., Repetto, M., Fernandez Pardal, M. M., Llesuy, S., and Poderoso, J. J. (1996). Neutrophil function, nitric oxide, and blood oxidative stress in Parkinson's disease. *Mov. Disord.* **11**, 261–267.

Grabert, K., Michoel, T., Karavolos, M. H., Clohisey, S., Baillie, J. K., Stevens, M. P., Freeman, T. C., Summers, K. M., and McColl, B. W. (2016). Microglial brain region-dependent diversity and selective regional sensitivities to aging. *Nat. Neurosci.* **19**, 504–516.

Greenamyre, J. T., Cannon, J. R., Drolet, R., and Mastroberardino, P. G. (2010). Lessons from the rotenone model of Parkinson's disease. *Trends Pharmacol. Sci.* **31**, 141–142. author reply 142–143.

Gustin, A., Kirchmeyer, M., Koncina, E., Felten, P., Losciuto, S., Heurtaux, T., Tardivel, A., Heuschling, P., and Dostert, C. (2015). NLRP3 Inflammasome is expressed and functional in mouse brain microglia but not in astrocytes. *PloS One* **10**, e0130624.

Halle, A., Hornung, V., Petzold, G. C., Stewart, C. R., Monks, B. G., Reinheckel, T., Fitzgerald, K. A., Latz, E., Moore, K. J., and Golenbock, D. T. (2008). The NALP3 inflammasome is involved in the innate immune response to amyloid-beta. *Nat. Immunol.* **9**, 857–865.

Heneka, M. T., Kummer, M. P., Stutz, A., Delekate, A., Schwartz, S., Vieira-Saecker, A., Griep, A., Axt, D., Remus, A., Tzeng, T. C., *et al.* (2013). NLRP3 is activated in Alzheimer's disease and contributes to pathology in APP/PS1 mice. *Nature* **493**, 674–678.

Hirsch, E. C., and Hunot, S. (2009). Neuroinflammation in Parkinson's disease: a target for neuroprotection? *Lancet Neurol.* **8**, 382–397.

Inden, M., Kitamura, Y., Abe, M., Tamaki, A., Takata, K., and Taniguchi, T. (2011). Parkinsonian rotenone mouse model: reevaluation of long-term administration of rotenone in C57BL/6 mice. *Biological & Pharmaceutical Bulletin* **34**, 92–96.

Johnson, M. E., and Bobrovskaya, L. (2015). An update on the rotenone models of Parkinson's disease: their ability to reproduce the features of clinical disease and model gene-environment interactions. *Neurotoxicology* **46**, 101–116.

Klein, C., and Westenberger, A. (2012). Genetics of Parkinson's disease. *Cold Spring Harb. Perspect. Med.* **2**, a008888.

Kolaczkowska, E., and Kubes, P. (2013). Neutrophil recruitment and function in health and inflammation. *Nat. Rev. Immunol.* **13**, 159–175.

Kreutzberg, G. W. (1996). Microglia: a sensor for pathological events in the CNS. *Trends in Neurosciences* **19**, 312–318.

Lue, L. F., Schmitz, C. T., Snyder, N. L., Chen, K., Walker, D. G., Davis, K. J., Belden, C., Caviness, J. N., Driver-Dunckley, E., Adler, C. H., *et al.* (2016). Converging mediators from immune and trophic pathways to identify Parkinson disease dementia. *Neurol. Neuroimmunol. Neuroinflamm.* **3**, e193.

McGeer, P. L., Itagaki, S., Boyes, B. E., and McGeer, E. G. (1988). Reactive microglia are positive for HLA-DR in the substantia nigra of Parkinson's and Alzheimer's disease brains. *Neurology* **38**, 1285–1291.

McGeer, P. L., Schwab, C., Parent, A., and Doudet, D. (2003). Presence of reactive microglia in monkey substantia nigra years after 1-methyl-4-phenyl-1,2,3,6-tetrahydropyridine administration. *Ann. Neurol.* **54**, 599–604.

Pan-Montojo, F., Anichtchik, O., Dening, Y., Knels, L., Pursche, S., Jung, R., Jackson, S., Gille, G., Spillantini, M. G., Reichmann, H., *et al.* (2010). Progression of Parkinson's disease pathology is reproduced by intragastric administration of rotenone in mice. *PloS One* **5**, e8762.

Pan-Montojo, F., Schwarz, M., Winkler, C., Arnhold, M., O'Sullivan, G. A., Pal, A., Said, J., Marsico, G., Verbavatz, J. M., Rodrigo-Angulo, M., *et al.* (2012). Environmental toxins trigger PD-like progression via increased alpha-synuclein release from enteric neurons in mice. *Sci. Rep.* **2**, 898.

Parillaud, V. R., Lornet, G., Monnet, Y., Privat, A. L., Haddad, A. T., Brochard, V., Bekaert, A., de Chanville, C. B., Hirsch, E. C., Combadiere, C., *et al.* (2017). Analysis of monocyte infiltration in MPTP mice reveals that microglial CX3CR1 protects against neurotoxic over-induction of monocyte-attracting CCL2 by astrocytes. *J. Neuroinflamm.* **14**, 60.

Pope, S. M., Zimmermann, N., Stringer, K. F., Karow, M. L., and Rothenberg, M. E. (2005). The eotaxin chemokines and CCR3 are fundamental regulators of allergen-induced pulmonary eosinophilia. *J. Immunol.* **175**, 5341–5350.

Qiao, C., Zhang, L. X., Sun, X. Y., Ding, J. H., Lu, M., and Hu, G. (2016). Caspase-1 deficiency alleviates dopaminergic neuronal death via inhibiting Caspase-7/AIF pathway in MPTP/p mouse model of Parkinson's disease. *Mol. Neurobiol.* doi:10.1007/s12035-016-9980-5.

Ross, C. A., and Smith, W. W. (2007). Gene-environment interactions in Parkinson's disease. *Parkinsonism Relat. Dis.* **13(Suppl 3)**, S309–S315.

Sarkar, S. N. P., Neal, M., Jin, H., Anantharam, V., Kanthasamy, A., and Kanthasamy, A. (2015). Pesticide-induced mitochondrial dysfunction augments NLRP3 inflammasome signaling pathway in primary microglia. *FASEB J.* **29**, 777.5.

Schroder, K., and Tschopp, J. (2010). The inflammasomes. *Cell* **140**, 821–832.

Sedgwick, J. D., Schwender, S., Imrich, H., Dorries, R., Butcher, G. W., and ter Meulen, V. (1991). Isolation and direct characterization of resident microglial cells from the normal and inflamed central nervous system. *Proc. Natl. Acad. Sci. U.S.A.* **88**, 7438–7442.

Shaftel, S. S., Carlson, T. J., Olschowka, J. A., Kyrkanides, S., Matousek, S. B., and O'Banion, M. K. (2007). Chronic interleukin-1beta expression in mouse brain leads to leukocyte infiltration and neutrophil-independent blood brain barrier permeability without overt neurodegeneration. *J. Neurosci.* **27**, 9301–9309.

Sherer, T. B., Betarbet, R., Kim, J. H., and Greenamyre, J. T. (2003). Selective microglial activation in the rat rotenone model of Parkinson's disease. *Neurosci. Lett.* **341**, 87–90.

Shiau, C. E., Monk, K. R., Joo, W., and Talbot, W. S. (2013). An anti-inflammatory NOD-like receptor is required for microglia development. *Cell Rep.* **5**, 1342–1352.

Singh, N. K., Banerjee, B. D., Bala, K., Chhillar, M., and Chhillar, N. (2014). Gene-gene and gene-environment interaction on the risk of Parkinson's disease. *Curr. Aging Sci.* **7**, 101–109.

Soehnlein, O., Steffens, S., Hidalgo, A., and Weber, C. (2017). Neutrophils as protagonists and targets in chronic inflammation. *Nat. Rev. Immunol.* **17**, 248–261.

Sofroniew, M. V. (2009). Molecular dissection of reactive astrogliosis and glial scar formation. *Trends Neurosci.* **32**, 638–647.

Sofroniew, M. V., and Vinters, H. V. (2010). Astrocytes: biology and pathology. *Acta Neuropathol.* **119**, 7–35.

Tanner, C. M. (1989). The role of environmental toxins in the etiology of Parkinson's disease. *Trends Neurosci.* **12**, 49–54.

Tanner, C. M., Kamel, F., Ross, G. W., Hoppin, J. A., Goldman, S. M., Korell, M., Marras, C., Bhudhikanok, G. S., Kasten, M., Chade, A. R., *et al.* (2011). Rotenone, paraquat, and Parkinson's disease. *Environ. Health Perspect.* **119**, 866–872.

Tieu, K. (2011). A guide to neurotoxic animal models of Parkinson's disease. *Cold Spring Harbor Perspectives in Medicine* **1**, a009316.

Valente, E. M., Abou-Sleiman, P. M., Caputo, V., Muqit, M. M., Harvey, K., Gispert, S., Ali, Z., Del Turco, D., Bentivoglio, A. R., Healy, D. G., *et al.* (2004). Hereditary early-onset Parkinson's disease caused by mutations in PINK1. *Science* **304**, 1158–1160.

Wild, E., Magnusson, A., Lahiri, N., Krus, U., Orth, M., Tabrizi, S. J., and Bjorkqvist, M. (2011). Abnormal peripheral chemokine profile in Huntington's disease. *PLoS Curr.* **3**, RRN1231.

Won, J. H., Park, S., Hong, S., Son, S., and Yu, J. W. (2015). Rotenone-induced impairment of mitochondrial electron transport chain confers a selective priming signal for NLRP3 inflammasome activation. *J. Biol. Chem.* **290**, 27425–27437.

Xu, Y., Sheng, H., Bao, Q., Wang, Y., Lu, J., and Ni, X. (2016). NLRP3 inflammasome activation mediates estrogen deficiency-induced depression- and anxiety-like behavior and hippocampal inflammation in mice. *Brain, Behav. Immun.* **56**, 175–186.

Yan, Y., Jiang, W., Liu, L., Wang, X., Ding, C., Tian, Z., and Zhou, R. (2015). Dopamine controls systemic inflammation through inhibition of NLRP3 inflammasome. *Cell* **160**, 62–73.

Zhang, Z. T., Du, X. M., Ma, X. J., Zong, Y., Chen, J. K., Yu, C. L., Liu, Y. G., Chen, Y. C., Zhao, L. J., and Lu, G. C. (2016). Activation of the NLRP3 inflammasome in lipopolysaccharide-induced mouse fatigue and its relevance to chronic fatigue syndrome. *J. Neuroinflamm.* **13**, 71.

Zhou, R., Yazdi, A. S., Menu, P., and Tschopp, J. (2011). A role for mitochondria in NLRP3 inflammasome activation. *Nature* **469**, 221–225.